land

MDPI

Article

Effect of the Belt and Road Initiatives on Trade and Its Related LUCC and Ecosystem Services of Central Asian Nations

Jian Zhang [1], Meixia Ren [1], Xin Lu [1], Yu Li [2] and Jianjun Cao [1,*]

[1] College of Geography and Environmental Science, Northwest Normal University, Lanzhou 730070, China; jianzhang@nwnu.edu.cn (J.Z.); 2020222757@nwnu.edu.cn (M.R.); 2021212899@nwnu.edu.cn (X.L.)
[2] School of Chemical Engineering, Northwest Minzu University, Lanzhou 730030, China; lifumeng@yahoo.com.cn
* Correspondence: caojj@nwnu.edu.cn

Abstract: Economic development and trade activities are some of the main driving forces leading to land use and land cover changes (LUCC) with impacts on ecosystem services (ESs) functions. As the origin of the Belt and Road Initiative (BRI) initiated by China, Central Asia nations (CANs) provide a prism to examine the impact of LUCC and ESs changes brought by the BRI. The impacts of LUCC and ecological influences were evaluated. The land use transfer matrix and dynamic index, the Vector Autoregressive (VAR) model, the Integrated Valuation of Ecosystem Services and Tradeoffs (InVEST), the Carnegie Ames–Stanford Approach (CASA) model, and the Revised Wind Erosion Equation (RWEQ) model were used to evaluate the impact of export trade from the CANs to China (ETCC) on LUCC and ESs in the CANs before and after the BRI. Results showed that before and after BRI (2001–2020), agricultural land and construction land increased by 59,120 km^2 and 7617 km^2, respectively, while ecological land decreased by 66,737 km^2. The annual growth rate of agricultural land and the annual reduction rate of ecological land after the BRI were higher than that before the BRI, while the annual growth rate of construction slowed down. Among the ecological land, the forestland increased by 5828 km^2 continuously, while the grassland increased by 12,719 km^2 and then decreased of 13,132 km^2. The trends for LUCC spatial variation were similar. The development of ETCC positively affected the changes in agricultural and construction land in the CANs and negatively affected the changes in ecological land. The average contribution rates of the ETCC to changes in agriculture, construction, and ecological lands after the BRI were higher than those before the BRI. They increased by 5.01%, 3.33% and 5.01%, respectively. The ESs after the BRI improved compared with those before the BRI, indicating that, during short-term implementation of the BRI, ETCC growth also ensures the ecological protection of CANs. This study provides a reference for dealing with trade, land management and environmental protection relations between member countries of international economic alliances worldwide.

Keywords: LUCC; economic trade; ecosystem services; Central Asia nations; Belt and Road Initiative

Citation: Zhang, J.; Ren, M.; Lu, X.; Li, Y.; Cao, J. Effect of the Belt and Road Initiatives on Trade and Its Related LUCC and Ecosystem Services of Central Asian Nations. *Land* **2022**, *11*, 828. https://doi.org/10.3390/land11060828

Academic Editor: Diane Pearson

Received: 27 April 2022
Accepted: 30 May 2022
Published: 1 June 2022

1. Introduction

China announced the plan for the construction of the Silk Road Economic Belt and the 21st Century Maritime Silk Road (known as the Belt and Road Initiative, BRI) in 2013, which immediately attracted attention worldwide [1–4]. The BRI associates Central and West Asia with the Persian Gulf and the Mediterranean, connecting Asia, Africa, and Europe [5]. The main aim of the BRI is to stimulate economic development of countries along the route [2]. However, with the implementation of the BRI, intense human economic activities may cause substantial disturbance to regional ecology and the environment of the BRI [6]. Research interest in the BRI regional economy and the ecological environment has increased [7–9]. Economic trade may lead to a decline in environmental quality [3,10,11] and the loss of ecosystem services (ESs) [12]. The environmental footprints of the BRI will likely continue to increase with economic growth and trade [13–16]. These reflect the increasing impact of international trade on the environmental sustainability of the BRI.

The influence of human economic activities on the regional ecosystems of the BRI is often accompanied by land use and land cover changes (LUCC) [9,17–19]. For example, with economic development, urban areas tend to expand rapidly and agricultural and ecological land is occupied [20]. Regional economic development needs the support of land, and LUCC has a strong influence on economic development. The needs of regional economic development and frequent trade activities are one of the main driving forces of LUCC [9,21]. In the terrestrial ecosystem assessment, land ESs are the most important element affecting the ecosystem quality [5]. ESs for assessing environmental change have usually been carried out based on LUCC [9]. Trade-driven LUCC significantly affect regional ecosystem structure and function, leading to landscape fragmentation and thus reduced ecosystem functions [22–25]. There is a need, therefore, to study LUCC driven by trade and their impacts on ecosystems in the BRI areas.

The Central Asia nations (CANs) are in a critical area of the Eurasian land bridge and form the strategic core region of the BRI [26,27]. The CANs are the main location for China to open up to the West [27]. The implementation of BRI projects has made China the core of the regional economy and the major trading partner with the CANs, comprising 25% of trade [28–30]. However, the CANs have a fragile ecological environment due to low levels of precipitation and a dry climate. They have also become known as "ecological hot spots" [31,32]. With the increase in regional land development intensity due to the trade activities of the BRI projects, the contradiction between human activity and natural ecology in the CANs has become increasingly prominent [33]. Hence, it is crucial for the CANs to ensure a sustainable ecological environment along with socioeconomic development [31].

Since the implementation of the BRI, most LUCC-based studies have focused on specific countries or smaller research areas [34]. There is still a lack of research on LUCC that encompasses multiple countries, especially trade-driven LUCC before and after the BRI. As the initiator of the BRI, China is the most important trading partner with the CANs. It is vital to study the changes in the export trade from the CANs to China (ETCC) and the resultant LUCC and changes in ESs. The objectives of this study were to examine (a) the impact of ETCC on LUCC in the CANs based on a Vector Autoregressive (VAR) model before and after the BRI and (b) to assess the ecological influences from changes in ESs induced by LUCC in the CANs before and after the BRI. This research can provide a baseline reference for land use decision-makers in countries along the BRI to formulate effective land use development and optimization policies, ensuring sustainable land use development and protecting the ecological environment.

2. Materials and Methods

2.1. Study Area

The CANs include the five republics of Kazakhstan (KAZ), Tajikistan (TJK), Uzbekistan (UZB), Turkmenistan (TKM), and Kyrgyzstan (KGZ) (Figure 1). The CANs are an important geographic center of the BRI and the birthplace of the BRI. The geographic position is between 35° N–55° N and 50° E–85° E with an area of approximately 400.8×10^4 km^2 with a population of 65 million [35,36]. The CANs are the world's largest arid and semi-arid region. There is a typical continental climate, with low levels of precipitation and a high diurnal temperature range. Regional water resources mainly comprise melting water from ice and snow on the mountains [31]. Distribution of water resources among the CANs countries is highly uneven. The oasis economy is the main development mode of the CANs, with agriculture playing a substantial role in the national economy. Agriculture in the region is based on plant production and animal husbandry [31]. Agricultural, construction, and ecological lands accounted for 21.07%, 0.21%, and 78.72%, respectively, of the land area in the CANs in 2013. The bilateral trade volume increased from US$460 million in 1992 to US$50.3 billion in 2013 [37].

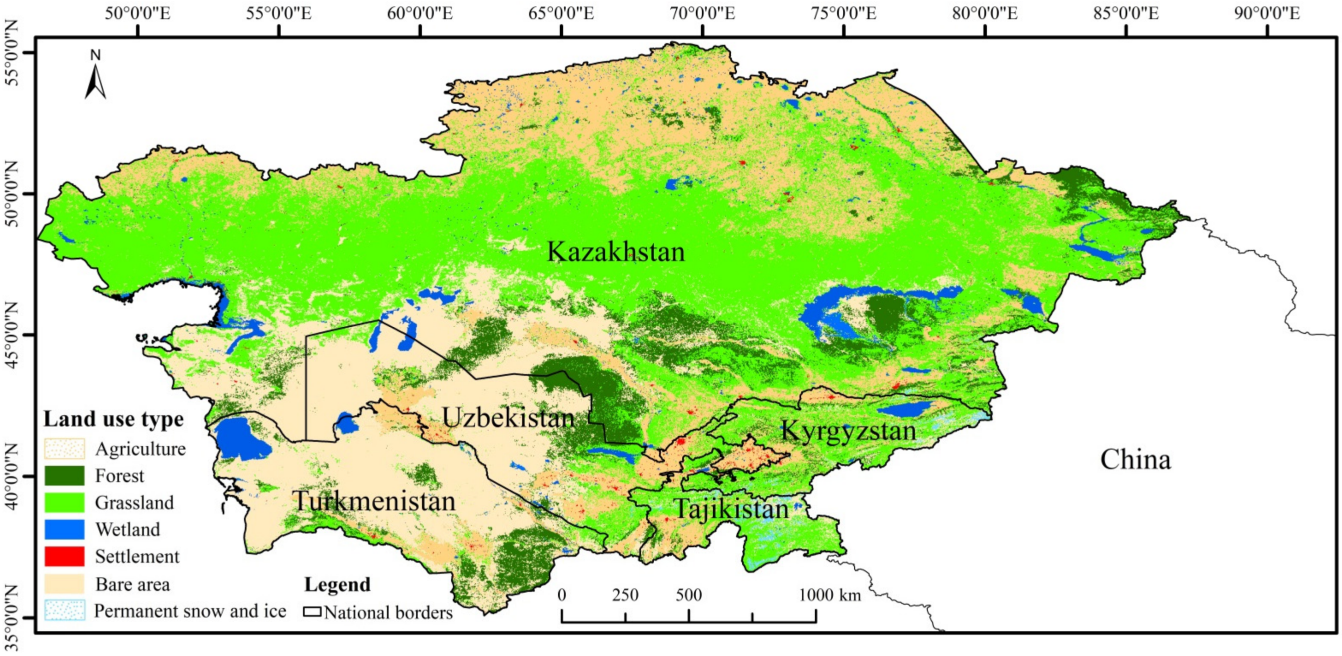

Figure 1. Geographical locations of the CANs.

2.2. Data Sources and Pre-Processing

In the present study, LUCC data and trade data were used to analyze the impact of ETCC on LUCC in the CANs based on the VAR model. LUCC data for the CANs areas with a resolution of 300 m was obtained from CCI-LC products in the European Space Agency (ESA) (https://www.esa-landcover-cci.org/, accessed on 26 October 2021) (Table 1). The LUCC data were divided into three categories, namely agricultural land (agriculture), construction land (settlement), and ecological land (forest, grassland, wetlands, and other land). The trade data between the CANs and China were obtained from the China Statistical Yearbook (http://www.stats.gov.cn/, accessed on 15 April 2021) (Table 1). The LUCC, climate, vegetation, terrain, and soil data were used to estimate the ecological consequences induced by LUCC in the CANs. Major ESs changes, including soil conservation, carbon sequestration, water yield, and wind erosion in the CANs, were assessed using multiple models for 2001, 2013, and 2020. Climate data including monthly average temperature and precipitation were obtained from Climatic Research Unit (CRU) (https://crudata.uea.ac.uk/cru/data/, accessed on 16 January 2021). The potential evapotranspiration and surface solar radiation were obtained from National Qinghai–Tibet Plateau Scientific Data Center (http://data.tpdc.ac.cn/, accessed on 30 March 2021). Daily climate data for the study area including temperature, precipitation, snow depth, and wind speed were collected from the global surface daily data summary of the National Centers for Environmental Information (https://www.ncdc.noaa.gov/, accessed on 4 November 2021). Spatial distribution maps of the daily climate data were obtained through Kriging interpolation. The digital elevation model (DEM) of the terrain data with a 1-km resolution was obtained from National Oceanic and Atmospheric Administration (NOAA) (https://www.ngdc.noaa.gov, accessed on 3 February 2021). The normalized difference vegetation index (NDVI) for the vegetation data was obtained from National Aeronautics and Space Administration (NASA) (https://search.earthdata.nasa.gov/, accessed on 15 May 2021). The soil data were obtained from the Harmonized World Soil Database (HWSD) v1.2 (http://www.fao.org/, accessed on 8 February 2021). All datasets were reprojected into the Albers coordinate system with a pixel size of 1 km × 1 km.

Table 1. Data sources.

Category	Data	Year	Resolution	Data Resource
LUCC	LUCC data	2001–2020	300 m	ESA (https://www.esa-landcover-cci.org/, accessed on 26 October 2021)
Climate (monthly)	Temperature Precipitation Potential evapotranspiration Surface solar radiation	1999–2001, 2011–2013, 2018–2020	50 km 10 km	CRU (https://crudata.uea.ac.uk/cru/data/, accessed on 16 January 2021) National Qinghai-Tibet Plateau Scientific Data Center (http://data.tpdc.ac.cn/, accessed on 30 March 2021)
Climate (daily)	Temperature precipitation snow depth wind speed	2001, 2013, 2020	1 km	Global surface summary of daily data of the National Centers for Environmental Information (https://www.ncdc.noaa.gov/, accessed on 4 November 2021)
Terrain	DEM	2010	1 km	NOAA (https://www.ngdc.noaa.gov/, accessed on 3 February 2021)
Vegetation	NDVI	2001, 2013, 2020	1 km	NASA (https://search.earthdata.nasa.gov/, accessed on 15 May 2021)
Soil	Soil data	2008	1 km	HWSD v1.2 (http://www.fao.org/, accessed on 8 February 2021)
Trade data	Total value of China customs goods import and export trade	2001–2020		China Statistical Yearbook (http://www.stats.gov.cn/, accessed on 15 April 2021).

Agricultural land, construction land, and ecological land were represented by AGR, CON, and ECO, respectively. To avoid substantial fluctuations in the time series data, the heteroscedasticity of the time series was eliminated to a certain extent by performing a natural logarithm (ln) transformation on the original data.

2.3. LUCC Transfer Matrix and Dynamic Index

The LUCC transfer matrix was used to present the conversion area from different LUCC types before and after the BRI, as follows [38]:

$$X = \begin{bmatrix} X_{11} & X_{12} & \cdots & X_{1j} \\ X_{21} & X_{21} & \cdots & X_{2j} \\ \vdots & \vdots & \ddots & \vdots \\ X_{i1} & X_{i2} & \cdots & X_{ij} \end{bmatrix} \quad (1)$$

where X_{ij} is the land area of transition from land use type i to j.

The formula for calculating the dynamic index of the land use type is as follows [39]:

$$K = \frac{U_b - U_a}{U_a} \times \frac{1}{T} \times 100\% \quad (2)$$

where U_a and U_b are the area of the land use type from the start time to the end time, respectively; T is the length of the period, measured in years; the K value represents the annual rate of change of a certain land use type during the study period.

2.4. VAR Model

The VAR model was proposed by Christopher Sims in 1980 and is currently the dominant economic research model [40]. It is one of the most successful, flexible and easy-to-use models for analyzing multivariate time series. It is a natural extension of univariate autoregressive models to dynamic multivariate time series. The model has proven particularly useful for describing the dynamic behavior of economic time series. One of the most important advantages of the model over general regression analysis its the avoidance of correlation and multicollinearity [40]. Currently, VAR models are mainly applied in terms of economic and financial fields [41–43]. There is a lack of research on the relationship between economy and land use. Therefore, to overcome the shortcomings of traditional methods, this study developed a VAR model that calculates the effect of ETCC on LUCC in the CANs (Figure 2). All operations of the model were implemented using EViews 10 software. The model is as follows [40]:

$$Y_t = A_1 Y_{t-1} + A_2 Y_{t-2} + \cdots + A_p Y_{t-p} + \varepsilon_t \tag{3}$$

where Y_t is the variable to be tested, denoting lnETCC, lnAGR, lnCON, and lnECO; ε_t is the random error term; p is the lag order; and $A_1, A_2, \cdots, A_p$ are the coefficient matrix to be tested.

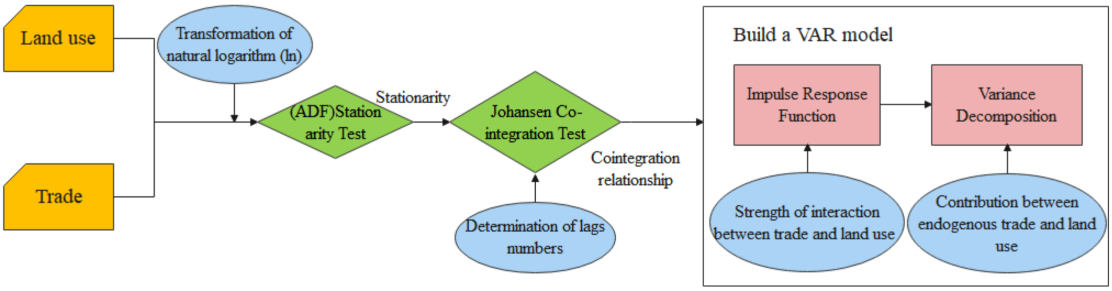

Figure 2. VAR model flow chart.

2.4.1. Unit Root Test (Stationarity Tests)

The standard method for checking the stationarity of a variable time series is to judge whether the unit root is stationary. In this study, the Augmented Dickey-Fuller (ADF) test method was used, which controls for higher-order serial correlation by adding the lagged differential term of the dependent variable Y_t to the right-hand side of the regression equation. This is done to test the stationarity of the lnETCC, lnAGR, lnCON, and lnECO [44]. The core expression is as follows:

$$\Delta Y_t = \alpha_0 + \alpha_1 Y_{t-1} + \alpha_2 t + \sum_{i=1}^{p} \gamma_i \Delta Y_{t-i} + \varepsilon_t \tag{4}$$

where α_i (i = 0, 1 and 2) represents the constant term; γ_i (i = 1, 2, ... , n) are the constant coefficients; t is the time variable; and p is the lag period, using the "t-sig" approach [45].

2.4.2. Impulse Response Function (IRF)

The IRF provided by the VAR model was used to identify the impact of ETCC on the LUCC and can generate time paths of LUCC due to trade shocks in the VAR model [46]. The function form is as follows [44]:

$$Y_t = \sum_{i=1}^{p} \alpha_{1i} Y_{t-i} + \sum_{i=1}^{p} \gamma_{1i} X_{t-i} + \varepsilon_{1t} \tag{5}$$

$$Y_t = \sum_{i=1}^{p} \alpha_{1i} Y_{t-i} + \sum_{i=1}^{p} \gamma_{1i} X_{t-i} + \varepsilon_{1t} \tag{6}$$

where ε_{1t}, ε_{2t} represents innovation, which is a random disturbance term. If ε_{1t} changes, the value of Y_t will change with the change of ε_{1t} at this time, and the current value of Y_t will affect the future values of X_t and Y_t. It can be observed how each variable in the system responds to change and other endogenous variables.

2.4.3. Variance Decomposition

The variance is used to measure the contribution of ETCC to LUCC, which is an acknowledged method used to study the relationship between the ETCC, AGR, CON, and ECO. This study performed the Variance Decomposition (VDM) analysis among the lnETCC, lnAGR, lnCON, and lnECO to determine the contribution of ETCC to LUCC. This could provide the relative degrees of the influence of various interference factors on the endogenous variables in the VAR model. An analysis of the VDM was undertaken according to a previous research method [47].

2.4.4. VAR Model Specification Tests

Beginning with the determination of the lag length, the optimal lag length was determined using three standard tests, namely the minimum Akaike information criterion, the Bayesian information criterion, and the Hannan–Quinn information criterion [46]. According to all three tests, the optimal lag order was 1. The existence of the co-integrating vectors was tested. If the ADF test and Johansen co-integration test confirm that the data are co-integrated at the level, it means that the specific VAR model is representative at this level.

2.5. Ecosystem Services Assessment

The CANs are located in an arid and semi-arid area with a little precipitation. The main habitat types are grassland and desert, and the ecological environment is fragile [47]. In recent years, research that assesses ESs in arid areas has gradually increased. These studies mainly seek to quantify ESs, such as soil conservation, wind erosion intensity, water yield, and carbon sequestration, in arid areas [48–50]. Water resources are the most critical limiting factor in arid regions, and water-related ESs should be considered. Therefore, four important sub-ESs, namely soil conservation (SC), carbon sequestration (CS), water yield (WY), and wind erosion (WE), were selected as the basis for ecosystem quality evaluation in this study. An Integrated Valuation of Ecosystem Services and Tradeoffs (InVEST), a Carnegie Ames–Stanford Approach (CASA), and a Revised Wind Erosion Equation (RWEQ) models were used to calculate the four sub-ESs. The ESs assessment methods are presented in Table 2.

Table 2. Ecosystem service assessment methods.

ESs Type	Model	Formula and Description	Reference
Soil conservation	Soil conservation module in InVEST	$SR = RKLS - USLE$ (7) $USLE = R \times K \times LS \times C \times P$ (8) $RKLS = R \times K \times LS$ (9) *SR* is the soil conservation amount (t·hm^{-2}); *USLE* is sediment retention (t·hm^{-2}); *RKLS* is the potential soil erosion (t·hm^{-2}); *R* is the rainfall erosivity (MJ·mm·hm^{-2}·h^{-1}); *K* in is the soil erodible factor (t·hm^{2}·h·hm^{-2}·MJ^{-1}·mm^{-1}); *LS, C* and *P* represent the slope length gradient, vegetation coverage and erosion management, respectively (dimensionless).	[51]
Carbon sequestration	CASA model	$NPP(x,t) = APAR(x,t) \times \varepsilon(x,t)$ (10) *NPP(x,t)* is the net primary production (gC·m^{-2}); *APAR(x,t)* is the absorbed photosynthetically active radiation (gC·m^{-2}·month^{-1}); *ε(x,t)* is actual light energy utilization (gC·MJ^{-1}); x and t represent the spatial location and time, respectively.	[52]
Water yield	Water yield module in InVEST	$Y_x = (1 - AET_x/P_x) \times P_x$ (11) Y_x is the water yield of grid *x* (mm). P_x is the annual average precipitation of grid *x* (mm). AET_x is the annual average actual evapotranspiration of grid *x* (mm).	[51]
Wind erosion intensity	RWEQ model	$SL = \frac{2x}{S^2} Q_{\max} \cdot e^{-(x/s)2}$ (12) $Q_{\max} = 109.8(WF \times EF \times SCF \times K \times COG)$ (13) $S = 150.71((WF \times EF \times SCF \times K \times COG)^{-0.3711}$ (14) *SL* is the amount of soil loss (kg· m^{-2}); *x* is the distance from non-erodible boundary (m); *S* is the critical field length (m); Q_{max} is the maximum transportation capacity (kg·m^{-1}); *WF* is the climate factor (kg·m^{-1}); *EF* is the soil erosion fraction (dimensionless); *SCF* is the soil crusting factor (dimensionless); K_0 is the soil roughness factor (dimensionless); *COG* is the comprehensive crop factor (dimensionless).	[53]

3. Results

3.1. The Development of Trade in the CANs with China Based on the BRI

From 2001 to 2020, the trade surplus in the CANs was maintained with China in 2001–2002 and 2011–2013, while the trend represented a trade deficit in 2003–2010 and 2014–2020 (Figure 3). Before the BRI, the total trade volume between the CANs and China grew rapidly, and the total import and export volume almost doubled after the BRI (Table 3, Figure 3). This trade balance gradually stabilized after the implementation of the BRI (Figure 3).

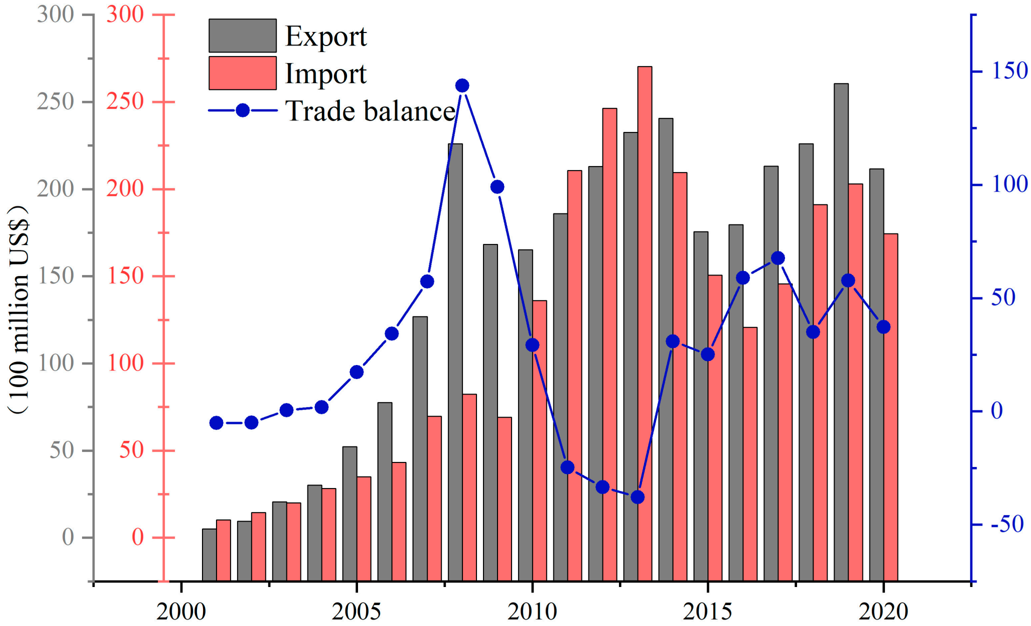

Figure 3. Changes in trade with China in the CANs from 2001 to 2020.

Table 3. CANs trade imports and exports from 2001 to 2020 (US$100 million).

Period	Total	Export Volume	Import Volume	Trade Balance
Before BRI	211.34	116.38	95.06	21.32
After BRI	386.03	215.34	170.69	44.65

3.2. Spatiotemporal Patterns of LUCC in CANs Based on BRI

From the LUCC conversion matrix (Table 4), the area of change before the BRI (2001–2013) was 139,721 km^2. This accounts for 3.49% of the total land, with an annual rate of change of 0.27%. The conversion between ecological land and agricultural land was the main change type, accounting for 22.65% of the total change. Agricultural land increased by 31,694 km^2, while ecological land decreased by 36,445 km^2 (Tables 4 and 6). Construction land increased by 4751 km^2, of which 3737 km^2 was from agriculture land and 1014 km^2 was from ecological land. Among the ecological land, there was an extensive conversion between grassland and other land. Since the BRI was implemented in 2013, the conversion matrix (Table 5) showed that 69,198 km^2 of the land underwent changes, which was far lower than that before the BRI. The conversion between ecological land and agricultural land were still the main change type, accounting for 39.63% of the total change. A total of 32,813 km^2 of ecological land was converted into agriculture land, while only 5387 km^2 of the agriculture land was converted into ecological land. A total of 2866 km^2 was converted into construction land, most of which had resulted from agriculture land conversion (64.62%). Among the ecological land, there was still extensive conversion between grassland and other land.

Table 4. LUCC conversion matrix in the CANs from 2001 to 2013 (unit: km^2).

2001	2013						2013 Total
	Agriculture	Forest	Grassland	Wetland	Settlement	Other	
Agriculture		953	10,248	74	3737	353	15,365
Forest	498		644	256	43	5	1446
Grassland	43,446	1989		163	850	2473	48,921
Wetland	674	785	1405		6	18671	21,541
Settlement							0
Other land	2441	13	49,343	536	115		52,448
2001 Total	47,059	3740	61,640	1029	4751	21,502	139,721

Table 5. LUCC conversion matrix in the CANs from 2013 to 2020 (unit: km^2).

2013	2020						2020 Total
	Agriculture	Forest	Grassland	Wetland	Settlement	Other	
Agriculture		1682	1527	303	1852	23	5387
Forest	158		338	57	27	4	584
Grassland	31,715	2022		445	808	1199	36,189
Wetland	176	388	232		1	1051	1848
Settlement							0
Other land	764	26	20,960	3262	178		25,190
2013 Total	32,813	4118	23,057	4067	2866	2277	69,198

In terms of the LUCC dynamic degree, the annual growth rate of agricultural land before and after the BRI was 0.32% and 0.46%, respectively. The annual growth rate of construction land before the BRI was 10.85%. However, the annual rate of change for construction land after the BRI was 4.87%, which was substantially slower (Table 6). Ecological land decreased by 0.10% and 0.14% before and after the BRI, respectively. After implementation of the BRI, the annual growth rate of forest is 0.14%, while that of grassland is 0.11% (Table 6).

Table 6. Dynamic changes of LUCC in the CANs from 2001 to 2020 (km^2).

LUCC Type	2001 (km^2)	2013 (km^2)	2020 (km^2)	Annual Rate of Change K (%) 2001–2013	Annual Rate of Change K (%) 2013–2020
Agricultural land	812,746	844,440	871,866	0.32%	0.46%
Construction land	3648	8399	11,265	10.85%	4.87%
Ecological land	3,192,079	3,155,634	3,125,342	−0.10%	−0.14%
Forest	355,091	357,385	360,919	0.06%	0.14%
Grassland	1,685,995	1,698,714	1,685,582	0.01%	−0.11%
Wetland	140,098	119,586	121,805	−1.22%	0.27%
Other	1,010,895	979,949	957,036	−0.26%	−0.33%

In terms of spatial distribution, the spatial analysis showed that the trends for LUCC were similar before and after implantation of the BRI (Figure 4). Before the BRI, the most pronounced changes occurred in the north and south parts of KAZ, and in the southeast part of UZB, as well as in the northwest part of KGZ, western part of TJK, and southern part of TKM. After the BRI, LUCC was less extensive compared with that before the BRI. When comparing before with after the BRI (Table 6), the extent of agricultural land increased rapidly, while ecological land rapidly decreased, with construction land increasing slowly in 2013–2020. Overall, from 2001 to 2020, the spatial change trend of LUCC was consistent with that before and after the BRI.

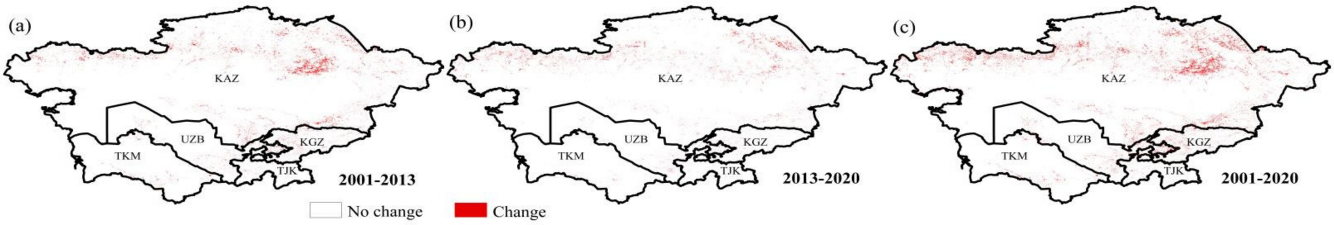

Figure 4. Spatial distribution of LUCC in the CANs from 2001 to 2013 (**a**), 2013–2020 (**b**) and 2001–2020 (**c**).

3.3. Response of LUCC to ETCC Based on BRI

There was evidence that the development of the ETCC slightly positively affected the changes in agriculture land and construction land in the CANs (Figure 5a,b). Agriculture land showed an increased response trend to ETCC before 2008, prior to a decreased response trend until the impact shock led to a convergent state after the BRI. Construction land showed a trend of increasing response to the ETCC before 2003 and then decreased rapidly until the response converged after the BRI. However, the ETCC slightly negatively affected the change in ecological land in the CANs (Figure 5c). Ecological land showed a decreasing response trend to the ETCC before 2008, prior to an increasing trend until the response reached a convergent state after the BRI.

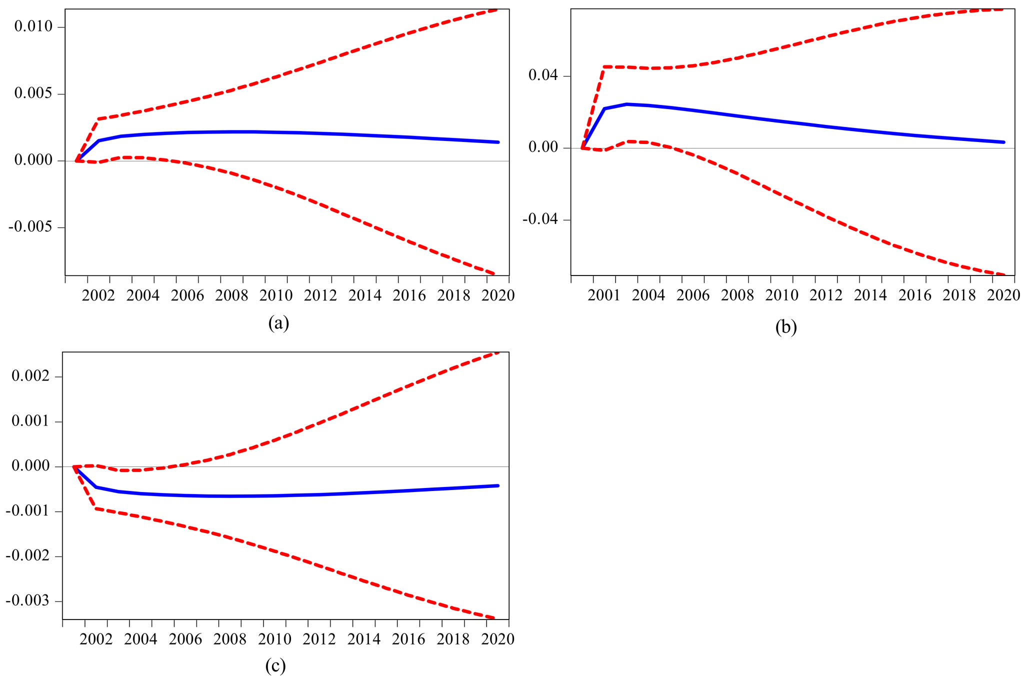

Figure 5. Response of LUCC to ETCC. (**a**) Response of lnAGR to lnETCC; (**b**) Response of lnCON to lnETCC; (**c**) Response of lnECO to lnETCC. Impulse: The ETCC expressed in 100 million US $ (±2 STD). Response: LUCC. The horizontal axis represents the tracking period of the IRF (unit: year) and the vertical axis represents the response degree of LUCC to ETCC. The solid blue line represents the IRF, that is, the trend of the variable after it has been affected. The dashed red line is the plus or minus twice the standard error of the trend.

With respect to the contribution of the ETCC to the LUCC (Table 7), the average contribution rates of ETCC to the changes in agriculture, construction, and ecological lands before the BRI were 7.21%, 6.95%, and 7.28%, respectively. The average contribution rates of ETCC to changes in agriculture, construction, and ecological lands after BRI increased to 12.22%, 10.28%, and 12.29%, respectively.

Table 7. Variance decomposition results of lnTRA, lnAGR, lnCON, and lnECO.

	Variance Decomposition of lnAGR					Variance Decomposition of lnCON				
Period	**S.E.**	**lnETCC**	**lnAGR**	**lnCON**	**lnECO**	**S.E.**	**lnETCC**	**lnAGR**	**lnCON**	**lnECO**
Average before BRI	0.01	7.21	80.47	0.54	11.78	0.18	6.95	71.15	15.99	5.91
Average after BRI	0.02	12.22	70.98	2.42	14.39	0.21	10.28	67.38	15.69	6.66
	Variance Decomposition of lnECO									
Period	**S.E.**	**lnETCC**	**lnAGR**	**lnCON**	**lnECO**					
Average before BRI	0.005	7.28	79.91	0.71	12.11					
Average after BRI	0.01	12.29	70.63	2.51	14.58					

3.4. Spatio-Temporal Patterns of Ecosystem Services

From 2001 to 2020, the spatial patterns of the four main ESs showed different trends in the CANs. SC exhibited an increasing spatial pattern in the CANs from northwest to southeast, while WE exhibited a decreasing trend from northwest to southeast. CS and WY exhibited an increasing trend from southwest to northeast (Figure 6).

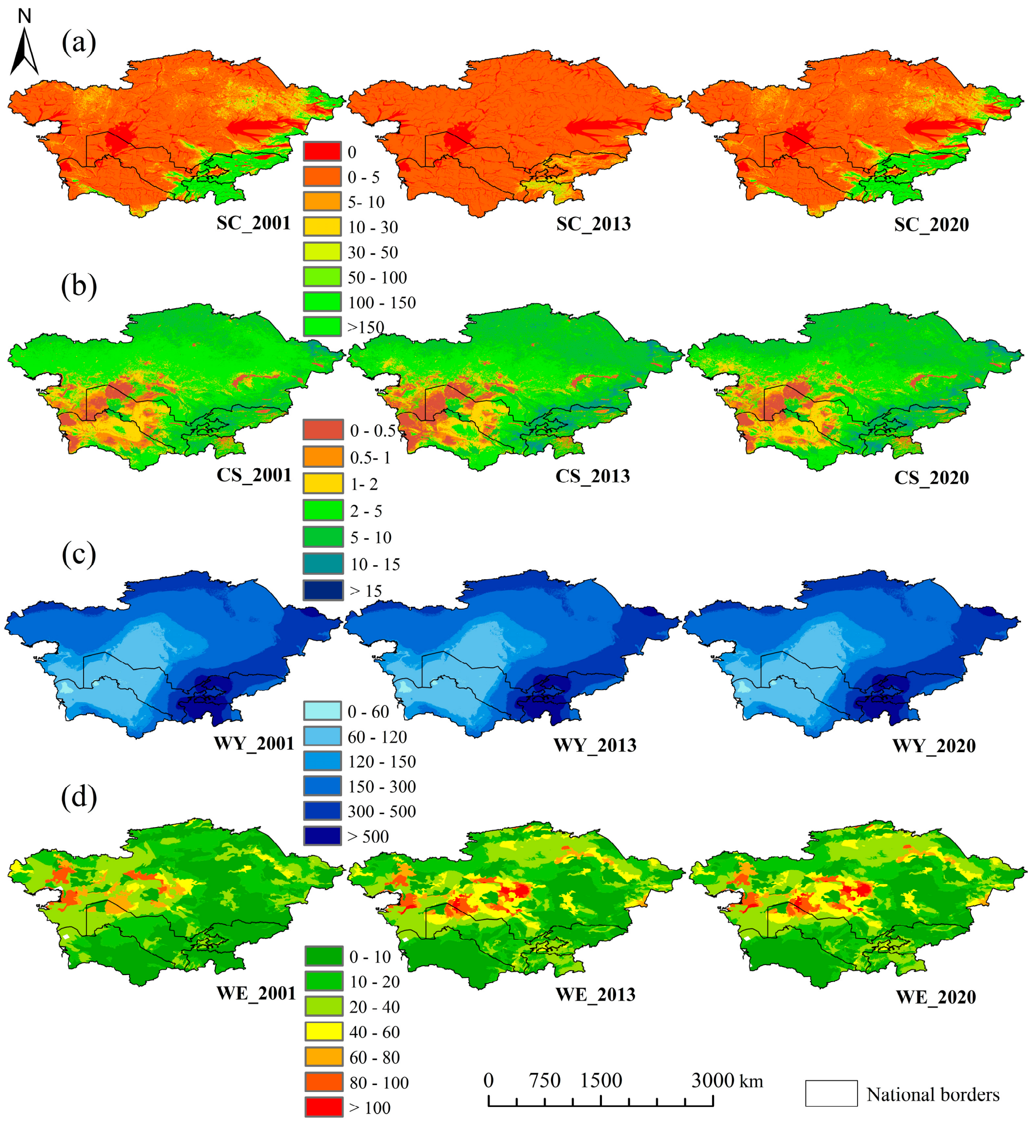

Figure 6. Spatial distribution of ESs in the CANs in 2001, 2013, and 2020. (**a**) SC; (**b**) CS; (**c**) WY; (**d**) WE. (SC, CS, WY, and WE refer to soil conservation, carbon sequestration, water yield, and wind erosion, respectively. The unit of SC and CS is t·hm^{-2}, of WE is kg·m^{-2}, and of WY is mm).

Comparing ESs before and after the BRI, before the BRI (2001–2013), SC exhibited a downward trend in most areas, and only a small part of the area exhibited an increasing trend, such as northwestern TJK and eastern KGZ (Figure 7). CS exhibited a stable or slightly decreasing trend in most regions and an increase in other regions, such as eastern and northern KAZ and most of KGZ. WY exhibited an increasing trend in most regions, and the remaining small regions exhibited a decreasing trend, such as in northern KAZ and most of TKM. WE exhibited an increasing trend in most areas, and the remaining small areas exhibited a decreasing trend, mainly in northwest KAZ. Since the implementation of the BRI (2013–2020), SC remained stable in most areas, with increases in a few areas, such as northern TJK and western KGZ, and decreases in some small areas, such as eastern TJK, eastern KGZ, and eastern KAZ (Figure 7). CS increased in most regions and decreased in only a few regions including western, southern, and eastern KGZ. WY showed an opposite trend to that before the BRI and decreased in most areas with an increase in other small areas. WE showed an opposite trend to that before the BRI, decreasing in most areas and increasing in other small areas that are mainly in KAZ (Figure 7). From 2001 to 2020, SC and CS showed similar trends to those before BRI. SC exhibited a downward trend in most areas, such as northwestern TJK. CS exhibited a stable or slightly decreasing trend in most regions. WY exhibited an increasing trend in some regions. It was mainly concentrated in the areas of TKM and UZB, as well as the central part of KAZ and the northwest part of TJK, and the remaining regions exhibited a decreasing trend. WE showed a similar change trend after BRI (Figure 7).

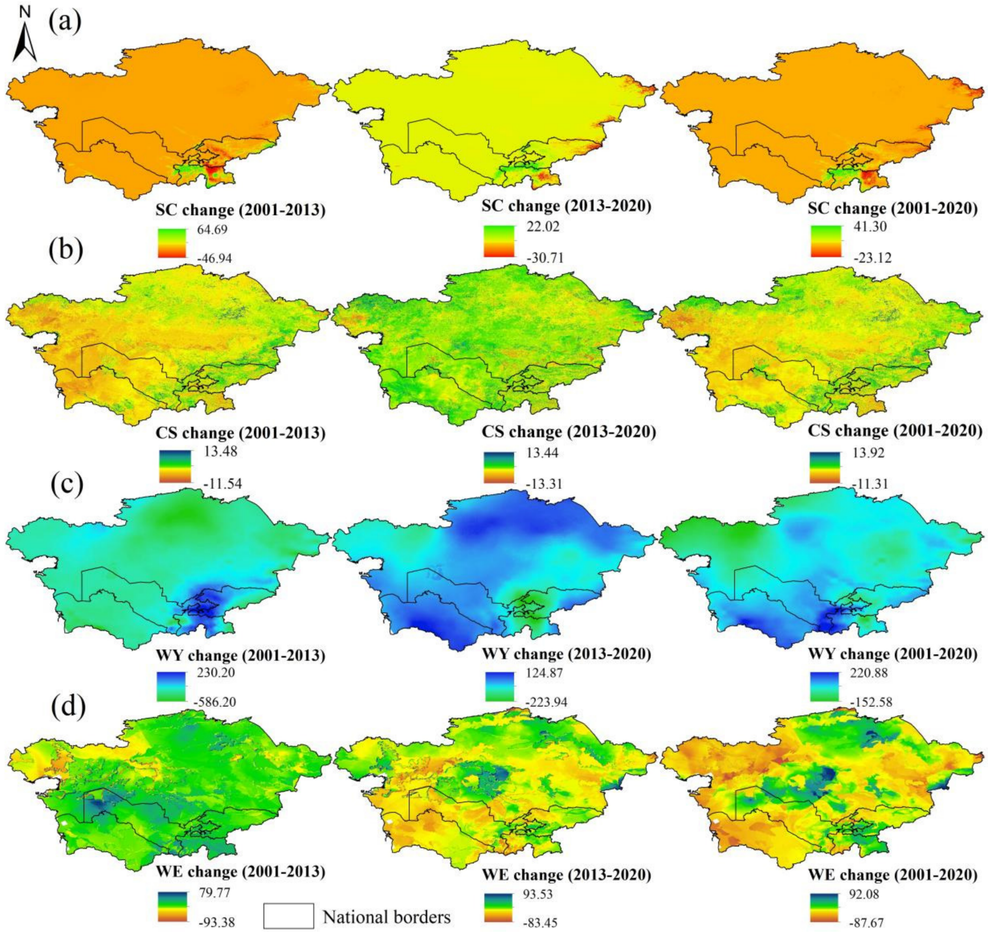

Figure 7. Spatial change in the ESs before BRI (2001–2013), after BRI (2013–2020) and 2001–2020. (**a**) SC change; (**b**) CS change; (**c**) WY change; (**d**) WE change. (SC, CS, WY, and WE refer to soil conservation, carbon sequestration, water yield, and wind erosion, respectively. The unit of SC and CS is t·hm^{-2}, of WE is kg·m^{-2}, and of WY is mm).

4. Discussion

4.1. Effect of ETCC on LUCC in the CANs

LUCC is usually constrained by population change, the urbanization level, and economic growth [54]. Population growth and economic expansion have always been key factors influencing LUCC [9], especially in developing countries such as the CANs. In the present study, findings showed that the increase in ETCC led to a continuous increase in the agriculture and construction land area and a continuous decrease in the ecological land area in the short term (Figure 5, Table 6). This suggested that ETCC was the main driver of LUCC in the CANs. This is in line with LUCC patterns of countries (such as CANs) that are driven by the demand for commodities from a country (such as China) with a strong economy and purchasing power [55]. This may be because international trade would affect the commodity supply and market price and thereby affect LUCC [56]. Trade has a long-term impact on the degradation of natural resources and changes in LUCC patterns [57]. When a country imports/exports goods, the land use may change, with the land used to be traded to produce these goods [58]. Variance decomposition results demonstrated that the contribution of the ETCC to LUCC after the BRI were higher than those before the BRI (Table 7), indicating that increased trade volumes have facilitated LUCC since the implementation of the BRI. Comparing the top 10 bulk commodities exported from the CANs to China before and after the BRI (Table 8), it was found that cereals, oil seeds, and oleaginous fruits were the fastest growing commodity in export trade besides mineral resources. Cereals are land intensive commodities [58]. The substantial increase in cereal exports from the CANs to China after the BRI had also directly resulted in a significant increase in agricultural land in the CANs.

Table 8. Comparison of the top 10 bulk commodities exported from the CANs to China before (2010) and after (2019) the BRI.

Commodity Name	Netweight (10^4 ton)		
	2010	2019	Changes
Mineral fuels, mineral oils and products of their distillation	1027.26	1145.05	117.79
Ores, slag and ash	668.05	262.37	−405.67
Iron and steel	69.88	103.31	33.44
Cereals	4.57	46.16	41.59
Oil seeds and oleaginous fruits	0.32	33.32	32.99
Copper and articles thereof	19.74	28.87	9.13
Salt; sulfur; earths and stone; plastering materials	138.24	19.79	−118.45
Residues and waste from the food industries	0.90	17.63	16.73
Zinc and articles thereof	6.71	14.17	7.46
Inorganic chemicals	1.38	12.16	10.78

Notes: Data was obtained from UN Comtrade Database (https://comtrade.un.org/data/, accessed on 25 March 2022).

The expansion of construction land before and after the BRI were indirectly affected by the ETCC because trade growth can directly promote the construction of logistics transportation corridors and population agglomeration. The increased construction land occupied agricultural land and ecological land, including towns, roads, and railways linking the agricultural areas, energy resources, and urban centers and towns in the CANs with China (Tables 4 and 5, Figure 4). Urban centers connected by transit corridors experienced significant expansion in the CANs after the BRI [30]. Urban areas increased by 32% via BRI road connections and 33% via BRI rail connections in KAZ [30]. Coupled with the reduction in rural populations from the transfer of the rural labor force to the cities and the rapid urbanization of the CANs due to the occupation of agricultural land by construction land, population agglomeration in urban and town areas further intensifies the expansion of construction land [30,59].

4.2. Impact of LUCC on ESs

LUCC driven by ETCC brought by the BRI has had a series of ecological influences on the CANs. In the present study, ecological land has decreased before and after the BRI due to the occupation of agricultural and construction lands. The annual reduction rate of ecological land after the BRI was higher than that before the BRI (Table 6). For the annual change rates of various types of ecological land before and after the BRI, forest showed a continuous increasing trend, while other land (mainly bare land) showed a continuous decreasing trend. Grassland increased and then decreased, whereas wetland decreased and then increased (Table 6). The substantial increase of forest before and after the BRI was consistent with the increasing trend of forest resources worldwide, as demonstrated by a range of studies [60,61]. However, this was likely related to the forest inventory from 2003 to 2013 and the forest management policies of the CANs [62]. Since the end of the last century, KAZ has acceded to the United Nations Convention to Combat Desertification, proposed a series of laws and regulations and adopted the concept of transition from forest management to sustainable development. As a result, the forest area expanded during the period 2005–2015 [3]. LUCC changed drastically from 2001 to 2020, and its evolution process had a certain impact on ESs in 2001, 2013 and 2020. In the areas where the LUCC changed, there were certain changes in ESs (Figure 7).

Changes in ecological land inevitably lead to changes in the ESs of the CANs. By comparing the changes of four main ESs in the CANs before and after BRI, it could be found that SC, CS, and WY in most areas before the BRI exhibited a downward trend, while the WE exhibited an upward trend. After the BRI, except the SC, which remained stable in most areas, the CS, WY, and WE in most areas were opposite to those before the BRI (Figure 7). The effects of LUCC on changes in ESs in the CANs before and after BRI are described in Table 9.

Table 9. Comparison of effect of LUCC on changes in ESs of the CANs before and after the BRI.

ES	Before BRI		After BRI	
	Trend	Explanation	Trend	Explanation
SC	Weak decline in most regions. Only a few regions exhibited an increasing trend	The conversion of agricultural land to grassland caused the weak decline in SC in most regions. Although the total area of grassland increased, the increased grassland was mainly in areas with low cover (<15%), while the reduced grassland was mainly in areas with high cover (Figure 4a) [51]. Only a few regions exhibited an increasing trend in SC, which was due to the decline in rainfall erosivity caused by the decrease of precipitation in these regions. The conversion from grassland to forest and other land (bare land) to grassland resulted in an increase in SC in mountainous regions [51]	Remained stable in most areas	The increase in SC in a few mountainous regions with higher altitude (such as the north of TJK and the west of KGZ) were related to the increase in small areas of forest. These results are in line with the results of Fu et al. [63] and Lu et al. [64]. There were also some higher altitude areas (such as eastern TJK, eastern KGZ, and eastern KAZ) where the decrease in SC was related to the increase in soil loss caused by the increase in precipitation.
CS	Weak decline in most regions	Consistent with the trends for SC	Upward trend in most areas	CS increased in the KGZ region. Forest has the most substantial impact on the functioning of the CS service [65]. We therefore conclude that the increase in CS in this region is because of the increase in forest land.
WY	Downward trend in most areas	The decline in WY in most areas was due to the increase in grassland, which mainly resulted from the conversion of agricultural land, wetland, and other land (bare land). When agricultural land was converted into grassland, the WY of the soil typically showed a downward trend [66]. Grassland decreased in regions with increased WY.	Upward trend in most areas	Grassland substantially decreased in most regions with increased WY, and forest in regions with reduced WY increased. The conversion from bare land to grassland and farmland has greatly reduced WY [51]. Changes in the ecosystem from low to high vegetation cover lead to an increase in evapotranspiration and a decrease in WY [51,67–70].

Table 9. *Cont.*

ES	Before BRI		After BRI	
	Trend	Explanation	Trend	Explanation
WE	Upward trend	The increase in WE in most regions was related to low grassland coverage (<15%). Even though the grassland area substantially increased, it did not play an important role in the change in WE [71]. Changes in other factors such as wind speed may have a more substantial impact on WE [72,73].	Downward trend in most areas	WE decreased in most regions, which was related to the increase in high coverage grassland. The spatial distribution pattern of the WE was consistent with the temperature variation pattern, and the WE increased with increasing temperature [73].

4.3. Implications for Land Use Management in CANs

Effective development planning is crucial for future land management and ESs improvement in the CANs. It is necessary to adjust the spatial distribution of agricultural and ecological lands according to local conditions, limit unplanned expansion of agricultural land, and ensure the integrity of ecological land and the supply of ESs. As an important corridor of the BRI [30], the CANs have moderately increased construction land while expanding transportation and logistics nodes, maintaining the service function of the ecological land. To formulate economic and trade development strategies, land planning and environmental protection policies in the future, the CANs should follow the principle of sustainable land development, which is often combined with the principle of the reasonable use of land resources [74]. Grasping the opportunities from the BRI, the CANs can implement protective projects for sustainable land management and improve awareness of comprehensive land resource management. This can provide policy makers with an important reference for environment protection and sustainable development in the CANs.

5. Conclusions

In this research, the CANs were chosen as the case study, and the impact of ETCC on LUCC in the CANs was quantified based on the VAR model before and after the BRI. The ecological influences from changes in ESs induced by LUCC in the CANs were assessed before and after the BRI. The main conclusions are as follows:

1. Before and after the BRI, agricultural and construction lands in the CANs increased to varying degrees, while ecological land decreased. The agricultural land increased by occupying the ecological land, while construction land increased by occupying agricultural land and ecological land. The annual growth rate of the agricultural land and the annual reduction rate in ecological land after the BRI were higher than that before the BRI. Meanwhile, the annual growth rate of construction land tended to slow down. On the ecological land, forest cover continuously increased, while the grassland increased and then decreased. The trends in LUCC spatial variation before and after the BRI were similar.
2. The development of ETCC had a weak positive impact on changes in agricultural and construction lands in the CANs and a weak negative impact on changes of ecological land in the CANs. The average contribution rates of the trade to the changes in agricultural, construction, and ecological lands in the CANs after the BRI were higher than those before the BRI.
3. SC, CS and WY in most areas of the CANs before the BRI exhibited a downward trend, while WE exhibited an upward trend. After the BRI, with the exception of SC in most areas, remained stable, CS, WY, and WE in most areas were opposite to those before the BRI. The ESs in the CANs after the BRI were improved compared with that before the BRI, indicating that during the short-term implementation of the BRI, ETCC growth also ensures the ecological protection of CANs.

This study provides a reference for dealing with trade, land management and environmental protection relations between member countries of international economic alliances worldwide, such as the European Union and the Association of Southeast Asian Nations. However, in this research, owing to the short implementation period of the BRI, the short-term impact of trade on the LUCC was relatively limited, and the long-term effect was uncertain. With the continuous promotion of the BRI, future studies should focus on the long-term impact of trade on the LUCC and ESs. The data on LUCC were from CCI-LC products in the ESA, and the spatial resolution was relatively low. The identification of the LUCC type area was not accurate enough, especially for the construction land, and the result was still uncertain. Higher resolution images should be used to improve the accuracy of the results in future research.

Author Contributions: Conceptualization, J.Z. and J.C.; methodology, M.R.; software, M.R. and X.L.; validation, J.Z., M.R. and J.C.; formal analysis, J.Z. and Y.L.; data curation, M.R. and X.L.; writing—original draft preparation, J.Z. and M.R.; writing—review and editing, J.Z., M.R. and Y.L.; supervision, J.C.; funding acquisition, Y.L. and J.C. All authors have read and agreed to the published version of the manuscript.

Funding: This research was funded by the Qilian Mountains Eco-environment Research Center in Gansu Province, Northwest Institute of Eco-environment and Resources, Chinese Academy of Sciences, grant number QLS202002, and the Arid Meteorological Science Research Fund Project in Gansu Province, China, grant number IAM202105.

Data Availability Statement: Not applicable.

Conflicts of Interest: The authors declare no conflict of interest.

Abbreviations

The following abbreviations are used in this manuscript:

LUCC	land use and land cover changes
ESs	ecosystem services
BRI	the Belt and Road Initiative
CANs	Central Asia nations
VAR	Vector Autoregressive
InVEST	Integrated Valuation of Ecosystem Services and Tradeoffs
CASA	Carnegie Ames–Stanford Approach
RWEQ	Revised Wind Erosion Equation
ADF	Augmented Dickey-Fuller
IRF	Impulse Response Function
VDM	Variance Decomposition
ETCC	export trade from the CANs to China
KAZ	Kazakhstan
TJK	Tajikistan
UZB	Uzbekistan
TKM	Turkmenistan
KGZ	Kyrgyzstan
AGR	agricultural land
CON	construction land
ECO	ecological land
SC	soil conservation
CS	carbon sequestration
WY	water yield
WE	wind erosion

References

1. Lin, J.Y. "One Belt and One Road" and free trade zones China's new opening-up initiatives. *Front. Econ. China* **2015**, *10*, 585–590.
2. Huang, Y. Understanding China's Belt & Road Initiative: Motivation, framework and assessment. *China Econ. Rev.* **2016**, *40*, 314–321.
3. Liu, G.; Nawab, A.; Meng, F.; Shah, A.M.; Deng, X.; Hao, Y.; Giannetti, B.F.; Agostinho, F.; Almeida, C.M.V.; Casazza, M. Understanding the Sustainability of the Energy–Water–Land Flow Nexus in Transnational Trade of the Belt and Road Countries. *Energies* **2021**, *14*, 6311. [CrossRef]
4. Shichor, Y. China's Belt and Road Initiative Revisited: Challenges and ways forward. *China Q. Int. Strat. Stud.* **2018**, *04*, 39–53. [CrossRef]
5. You, Y.; Zhou, N.; Wang, Y. Comparative study of desertification control policies and regulations in representative countries of the Belt and Road Initiative. *Glob. Ecol. Conserv.* **2021**, *27*, e01577. [CrossRef]
6. Yang, R.; Bai, Z.; Pan, J.; Zhang, J.; Liu, X. Ecological risk analysis of countries along the belt and road based on LUCC: Taking Kuwait as a typical case. *Acta Ecol. Sin.* **2021**. [CrossRef]
7. Yang, R.; Meng, W.; Duan, N.; Shu, J.; Zhang, H. Ecological Civilization Construction Strategies in the Tianshan Mountain Northern Slope Economic Belt. *Strateg. Study Chin. Acad. Eng.* **2017**, *19*, 40.
8. Hafeez, M.; Chunhui, Y.; Strohmaier, D.; Ahmed, M.; Jie, L. Doesfinance affect environmental degradation: Evidence from One Belt and One Road Initiative region? *Environ. Sci. Pollut. Res.* **2018**, *25*, 9579–9592. [CrossRef]
9. Zuo, Q.; Li, X.; Hao, L.; Hao, M. Spatiotemporal Evolution of Land-Use and Ecosystem Services Valuation in the Belt and Road Initiative. *Sustainability.* **2020**, *12*, 6583. [CrossRef]
10. Enderwick, P. The economic growth and development effects of China's One Belt, One Road Initiative. *Strateg. Chang.* **2018**, *27*, 447–454. [CrossRef]
11. Tian, X.; Geng, Y.; Sarkis, J.; Zhong, S. Trends and features of embodied flows associated with international trade based on bibliometric analysis. *Resour. Conserv. Recycl.* **2018**, *131*, 148–157. [CrossRef]
12. Poelmans, L.; Van Rompaey, A. Complexity and performance of urban expansion models. *Comput. Environ. Urban Syst.* **2010**, *34*, 17–27. [CrossRef]
13. Fang, K.; Wang, S.; He, J.; Song, J.; Fang, C.; Jia, X. Mapping the environmental footprints of nations partnering the Belt and Road Initiative. *Resour Conserv Recycl.* **2021**, *164*, 105068. [CrossRef]
14. Alam, M.M.; Murad, M.W.; Noman AH, M.; Ozturk, I. Relationships among carbon emissions, economic growth, energy consumption and population growth: Testing Environmental Kuznets Curve hypothesis for Brazil, China, India and Indonesia. *Ecol. Indic.* **2016**, *70*, 466–479. [CrossRef]
15. Rauf, A.; Liu, X.; Amin, W.; Ozturk, I.; Rehman, O.U.; Hafeez, M. Testing EKC hypothesis with energy and sustainable development challenges: A fresh evidence from belt and road initiative economies. *Environ. Sci. Pollut. Res.* **2018**, *25*, 32066–32080. [CrossRef]
16. Solarin, S.A.; Bello, M.O. Persistence of policy shocks to an environmental degradation index: The case of ecological footprint in 128 developed and developing countries. *Ecol. Indicat.* **2018**, *89*, 35e44. [CrossRef]
17. Wolff, S.; Schulp, C.J.; Verburg, P.H. Mapping ecosystem services demand: A review of current research and future perspectives. *Ecol. Indic.* **2015**, *55*, 159–171. [CrossRef]
18. Liu, W.; Zhan, J.; Zhao, F.; Yan, H.; Zhang, F.; Wei, X. Impacts of urbanization-induced land-use changes on ecosystem services: A case study of the Pearl River Delta Metropolitan Region, China. *Ecol. Indic.* **2019**, *98*, 228–238. [CrossRef]
19. Baniya, S.; Rocha, N.; Ruta, M. Trade effects of the New Silk Road: A gravity analysis. *J. Dev. Econ.* **2020**, *146*, 102467. [CrossRef]
20. Rahmonov, O.; Abramowicz, A.; Pukowiec-Kurda, K.; Fagiewicz, K. The link between a high-mountain community and ecosystem services of juniper forests in Fann Mountains (Tajikistan). *Ecosyst. Serv.* **2021**, *48*, 101255. [CrossRef]
21. Grainger, A.; Konteh, W. Autonomy, ambiguity and symbolism in African politics: The development of forest policy in Sierra Leone. *Land Use Policy* **2007**, *24*, 42–61. [CrossRef]
22. Adnan, M.; Abdullah, A.; Dewan, A.; Hall, J.W. The effects of changing land use andflood hazard on poverty in coastal Bangladesh. *Land Use Policy* **2020**, *99*, 104868. [CrossRef]
23. Byun, E.; Sato, H.; Cowling, S.A. Extensive wetland development in mid-latitude North America during the Bølling-Allerød. *Nat. Geosci.* **2020**, *14*, 30–35. [CrossRef]
24. Dadashpoor, H.; Azizi, P.; Moghadasi, M. Land use change, urbanization, and change in landscape pattern in a metropolitan area. Sci. *Total Environ.* **2019**, *655*, 707–719. [CrossRef]
25. Santos-Martín, F.; Zorrilla-Miras, P.; Palomo, I.; Montes, C.; Benayas, J.; Maes, J. Protecting nature is necessary but not sufficient for conserving ecosystem services: A comprehensive assessment along a gradient of land-use intensity in Spain. *Ecosyst. Serv.* **2019**, *35*, 43–51. [CrossRef]
26. Li, P.; Qian, H.; Howard, K.W.; Wu, J. Building a new and sustainable "Silk Road economic belt". *Environ. Earth Sci.* **2015**, *74*, 7267–7270. [CrossRef]
27. Huang, J.; Na, Y.; Guo, Y. Spatiotemporal characteristics and driving mechanism of the coupling coordination degree of urbanization and ecological environment in Kazakhstan. *J. Geogr. Sci.* **2020**, *30*, 1802–1824. [CrossRef]
28. Aminjonov, F.; Abylkasymova, A.; Aimée, A.; Eshchanov, B.; Moldokanov, D.; Overland, I.; Vakulchuk, R. *BRI in Central Asia: Overview of Chinese Projects*; NUPI: Houston, TX, USA, 2019; pp. 1–5.

29. Kokushkina, I.; Soloshcheva, M. The role of central Asia in the"One Belt—One Road" initiative. *Iran Cauc.* **2019**, *23*, 283–298. [CrossRef]
30. Sternberg, T.; McCarthy, C.; Hoshino, B. Does China's Belt and Road Initiative Threaten Food Security in Central Asia? *Water* **2020**, *12*, 2690. [CrossRef]
31. Li, J.X.; Chen, Y.N.; Xu, C.C.; Li, Z. Evaluation and analysis of ecological security in arid areas of Central Asia based on the emergy ecological footprint (EEF) model. *J. Clean. Prod.* **2019**, *235*, 664–677. [CrossRef]
32. Robinson, S.; Kerven, C.; Behnke, R.; Kushenov, K.; Milner-Gulland, E.J. Pastoralists as optimal foragers? Reoccupation and site selection in the deserts of post-soviet Kazakhstan. *Hum. Ecol. Sci.* **2017**, *45*, 5–21. [CrossRef]
33. Reyer, C.; Otto, I.; Adams, S.; Albrecht, T.; Baarsch, F.; Cartsburg, M.; Coumou, D.; Eden, A.; Ludi, E.; Marcus, R.; et al. Climate change impacts in Central Asia and their implications for development. Reg. *Environ. Chang.* **2017**, *17*, 1639–1650. [CrossRef]
34. Camacho-Valdéz, V.; Ruiz-Luna, A.; Ghermandi, A.; Nunes, P.A.L.D.; Ruiz-Luna, A. Valuation of ecosystem services provided by coastal wetlands in northwest Mexico. *Ocean Coast. Manag.* **2013**, *78*, 1–11. [CrossRef]
35. Li, J.; Chen, H.; Zhang, C.; Pan, T. Variations in ecosystem service value in response to land use/land cover changes in Central Asia from 1995–2035. *PeerJ* **2019**, *7*, e7665. [CrossRef]
36. Hamidov, A.; Helming, K.; Balla, D. Impact of agricultural land use in Central Asia: A review. *Agron Sustain Deva.* **2016**, *36*, 6. [CrossRef]
37. Nie, L. An analysis of economic and trade cooperation between China and Central Asian countries in the context of "One Belt, One Road". *Mod. Commun.* **2018**, *4*, 78–81. (In Chinese)
38. Li, H.; Wang, J.; Zhang, J.; Qin, F.; Hu, J.; Zhou, Z. Analysis of characteristics and driving factors of wetland landscape pattern change in Henan Province from 1980 to 2015. *Land* **2021**, *10*, 564. [CrossRef]
39. Wang, Y.; Dai, E.; Yin, L.; Ma, L. Land use/land cover change and the effects on ecosystem services in the Hengduan Mountain region, China. *Ecosyst. Serv.* **2018**, *34*, 55–67. [CrossRef]
40. Zhou, D.T.; Yu, H.Y.; Li, Z.G. Effects of fluctuations in international oil prices on China's price level based on VAR model. *J. Discret. Math. Sci. Cryptogr.* **2017**, *20*, 125–135. [CrossRef]
41. Yazdi, S.K.; Shakouri, B.T. The renewable energy, CO_2 emissions, and economic growth: VAR model. *Energ Source Part B* **2018**, *13*, 53–59. [CrossRef]
42. Piroli, G.; Ciaian, P. Land use change impacts of biofuels: Near-VAR evidence from the US. *Ecol. Econ.* **2012**, *84*, 98–109. [CrossRef]
43. Zhao, J.; Mu, X.; Gao, P. Dynamic response of runoff to soil and water conservation measures and precipitation based on VAR model. *Hydrol Res.* **2019**, *50*, 837–848. [CrossRef]
44. Groenewold, N.; Guoping, L.; Anping, C. Regional output spillovers in China: Estimates from a VAR model. *Pap. Reg. Sci.* **2007**, *86*, 101–122. [CrossRef]
45. Hall, A. Testing for a unit root in time series with pretest data-based model selection. *J. Bus Econ. Stat.* **1994**, *12*, 461–470.
46. Sasikumar, R.; Abdullah, A.S. Vector autoregressive approach for impact of oil India stock price on fuel price in India. *Commun. Stat. Case Stud. Data Anal. Appl.* **2017**, *3*, 41–47. [CrossRef]
47. Rafiq, S.; Salim, R.; Bloch, H. Impact of crude oil price volatility on economic activities: An empirical investigation in the Thai economy. *Resour. Policy* **2009**, *34*, 121–132. [CrossRef]
48. Chen, Y.; Yue, W.; Liu, X.; Zhang, L.; Chen, Y.A. Multi-Scenario Simulation for the Consequence of Urban Expansion on Carbon Storage: A Comparative Study in Central Asian Republics. *Land* **2021**, *10*, 608. [CrossRef]
49. Jia, X.; Fu, B.; Feng, X.; Hou, G.; Liu, Y.; Wang, X. The tradeoff and synergy between ecosystem services in the Grain-for-Green areas in Northern Shaanxi, China. *Sci. Total Environ.* **2014**, *43*, 103–113. [CrossRef]
50. Dong, X.; Yang, W.; Ulgiati, S.; Yan, M.; Zhang, X. The impact of human activities on natural capital and ecosystem services of natural pastures in North Xinjiang, China. *Ecol. Modell.* **2012**, *225*, 28–39. [CrossRef]
51. Fu, Q.; Li, B.; Hou, Y.; Bi, X.; Zhang, X. Effects of land use and climate change on ecosystem services in Central Asia's arid regions: A case study in Altay Prefecture, China. *Sci. Total Environ.* **2017**, *607*, 633–646. [CrossRef]
52. Kelong, C.; Yanli, H.; Shengkui, C.; Jin, M.; Guangchao, C.; Hui, L. The study of vegetation carbon storage in Qinghai Lake Valley based on remote sensing and CASA model. *Procedia Environ. Sci.* **2011**, *10*, 1568–1574. [CrossRef]
53. Yang, G.; Sun, R.; Jing, Y.; Xiong, M.; Li, J.; Chen, L. Global assessment of wind erosion based on a spatially distributed RWEQ model. *Prog. Prog. Phys. Geog.* **2021**, *46*, 1. [CrossRef]
54. Wenhui, K. Analysis of Land Use and Coverage Change (LUCC) and Its Driving Mechanisms in Shanxi Province: Integrating Remotely Sensed Information and the Scientific Literature. *Resour. Sci.* **2011**, *33*, 1621–1629.
55. Meyfroidt, P.; Lambin, E.F.; Erb, K.H.; Hertel, T.W. Globalization of land use: Distant drivers of land change and geographic displacement of land use. *Curr. Opin. Environ. Sustain.* **2013**, *5*, 438–444. [CrossRef]
56. Millington, J.D.; Xiong, H.; Peterson, S.; Woods, J. Integrating modelling approaches for understanding telecoupling: Global food trade and local land use. *Land* **2017**, *6*, 56. [CrossRef]
57. Würtenberger, L.; Koellner, T.; Binder, C.R. Virtual land use and agricultural trade: Estimating environmental and socio-economic impacts. *Ecol. Econ.* **2006**, *57*, 679–697. [CrossRef]
58. Zhang, J.; Zhao, N.; Liu, X.; Liu, Y. Global virtual-land flow and saving through international cereal trade. *J. Geogr. Sci.* **2016**, *26*, 619–639. [CrossRef]

59. Lambin, E.F.; Meyfroidt, P. Global land use change, economic globalization, and the looming land scarcity. *Proc. Natl. Acad. Sci. USA* **2011**, *108*, 3465. [CrossRef]
60. Adams, M.A.; Pfautsch, S. Grand Challenges: Forests and Global Change. *Front. For. Glob. Chang.* **2018**, *1*, 1. [CrossRef]
61. FAO. State of the World's Forests 2016. Forests and agriculture: Land-use challenges and opportunities. Food Agric. *Organ. U. N. Rome* **2016**, *63*, 105–107.
62. MacDicken, K.G.; Sola, P.; Hall, J.E.; Sabogal, C.; Tadoum, M.; de Wasseige, C. Global progress toward sustainable forest management. *For. Ecol. Manag.* **2015**, *352*, 47–56. [CrossRef]
63. Fu, B.; Liu, Y.; Lü, Y.; He, C.; Zeng, Y.; Wu, B. Assessing the soil erosion control service of ecosystems change in the Loess Plateau of China. *Ecol. Complex.* **2011**, *8*, 284–293. [CrossRef]
64. Lü, Y.; Fu, B.; Feng, X.; Zeng, Y.; Liu, Y.; Chang, R.; Sun, G.; Wu, B. A policy-driven large scale ecological restoration: Quantifying ecosystem services changes in the Loess Plateau of China. *PLoS ONE* **2012**, *7*, e31782.
65. Wang, D.; Wang, B.; Niu, X. Forest carbon sequestration in China and its benefits. *Scand. J. For. Res.* **2014**, *29*, 51–59. [CrossRef]
66. Wang, X.; Bennett, J. Policy analysis of the conversion of cropland to forest and grassland program in China. *Environ. Econ Policy.* **2008**, *9*, 119–143. [CrossRef]
67. Wang, Z.; Mao, D.; Li, L.; Jia, M.; Dong, Z.; Miao, Z.; Ren, C.; Song, C. Quantifying changes in multiple ecosystem services during 1992–2012 in the Sanjiang Plain of China. *Sci. Total Environ.* **2015**, *514*, 119–130. [CrossRef]
68. Liu, M.; Tian, H.; Chen, G.; Ren, W.; Zhang, C.; Liu, J. Effects of land-use and land-cover change on evapotranspiration and water yield in China during 1900—2000. *J. Am. Water Resour. As.* **2008**, *44*, 1193–1207. [CrossRef]
69. López-Moreno, J.I.; Vicente-Serrano, S.M.; Moran-Tejeda, E.; Zabalza, J.; Lorenzo-Lacruz, J.; García-Ruiz, J.M. Impact of climate evolution and land use changes on water yield in the Ebro basin. *Hydrol. Earth Syst. Sci.* **2011**, *15*, 311–322. [CrossRef]
70. Gao, J.; Li, F.; Gao, H.; Zhou, C.; Zhang, X. The impact of land-use change on water-related ecosystem services: A study of the Guishui River Basin, Beijing, China. *J. Clean. Prod.* **2017**, *163*, S148–S155. [CrossRef]
71. Zhao, Y.; Wu, J.; He, C.; Ding, G. Linking wind erosion to ecosystem services in drylands: A landscape ecological approach. *Landsc Ecol.* **2017**, *32*, 2399–2417. [CrossRef]
72. Zhang, G.; Azorin-Molina, C.; Shi, P.; Lin, D.; Guijarro, J.A.; Kong, F.; Chen, D. Impact of near-surface wind speed variability on wind erosion in the eastern agropastoral transitional zone of Northern China, 1982–2016. *Agric. For. Meteorol.* **2019**, *2*, 039.
73. Teng, Y.; Zhan, J.; Liu, W.; Sun, Y.; Agyemang, F.B.; Liang, L.; Li, Z. Spatiotemporal dynamics and drivers of wind erosion on the Qinghai-Tibet Plateau, China. *Ecol. Indic.* **2021**, *123*, 107340.
74. Shigaeva, J.; Wolfgramm, B.; Dear, C. *Sustainable Land Management in Kyrgyzstan and Tajikistan: A Research Review*; UCA: Farnham, UK, 2013; p. 92.